SPOrt: an Experiment Aimed at Measuring the Large Scale Cosmic Microwave Background Polarization

Ettore Carretti,[a] Stefano Cortiglioni,[a] Gianni Bernardi,[a] Stefano Cecchini,[a] Claudio Macculi,[a] Carla Sbarra,[a] Jader Monari,[b] Alessandro Orfei,[b] Marco Poloni,[b] Sergio Poppi,[b] Giuliano Boella,[c] Silvio Bonometto,[c] Massimo Gervasi,[c] Giorgio Sironi,[c] Mario Zannoni,[d] Marco Tucci,[e] Massimo Baralis,[f] Oscar A. Peverini,[f] Riccardo Tascone,[f] Giuseppe Virone,[f] Roberto Fabbri,[g] Luciano Nicastro,[h] Kin-Wang Ng,[i] V.A. Razin,[j] Evgenij N. Vinyajkin,[j] Mikhail V. Sazhin,[k] Igor A. Strukov[l]

[a]IASF/CNR Sezione di Bologna, Via Gobetti 101, I-40129 Bologna, Italy
[b]IRA/CNR, Via Gobetti 101, I-40129, Bologna, Italy
[c]Dip. di Fisica, Univ. di Milano - Bicocca, P.za della Scienza 3, I–20126 Milano, Italy
[d]IASF/CNR Sezione di Milano, Via Bassini 15, I-20133 Milano, Italy
[e]Instituto de Fisica de Cantabria, Avda Los Castros s/n, 39005 Santander, Spain
[f]IRITI/CNR, c.so Duca degli Abruzzi 24, I–10129 Torino, Italy
[g]Dip. di Fisica, Univ. di Firenze, Via Sansone 1, I–50019 Sesto Fiorentino (FI), Italy
[h]I.A.S.F./C.N.R. Sez. di Palermo, via U. La Malfa 153, I–90146 Palermo, Italy
[i]Academia Sinica, 11529 Taipei, Taiwan
[j]NIRFI, 25 B.Pecherskaya st., Nizhnij Novgorod 603600/GSP-51, Russia
[k]Schternberg Astronomical Institute, Moscow State University, Moscow 119899, Russia
[l]IKI, Profsojuznaja ul. 84/32, Moscow 117810, Russia

ABSTRACT

SPOrt (Sky Polarization Observatory) is a space experiment aimed at measuring the microwave polarized emission in the frequency range 22-90 GHz with HPBW=7°. The Galactic polarized emission can be observed at the lower frequencies as well as the polarization of the Cosmic Microwave Background (CMB) at 90 GHz, where contaminants are expected to be lower. The extremely low level of the CMB Polarization signal ($< 1\ \mu$K) calls for intrinsically stable radiometers. The SPOrt instrument is expressly devoted to CMB polarization measurements and the whole design has been optimized for minimizing the instrumental polarization effects. In this contribution we present the receiver architecture based on correlation techniques, the analysis showing its intrinsic stability and the custom hardware development carried out to detect so low signal. SPOrt in an ASI funded project selected by ESA to be flown on the International Space Station during Early Utilization Phase.

Keywords: CMB, Polarization, Polarimeter, Instrumental Effects

1. INTRODUCTION

The Cosmic Microwave Background (CMB) is a powerful tool to understand origin and evolution of the Universe. The hot Big Bang model foresees the CMB as a Black Body radiation almost isotropic and unpolarized. Nevertheless, any deviations from this ideal behaviour is related to the cosmological parameters allowing their determination.[1–4] Very small CMB Anisotropy (CMBA) has been detected at both large[5,6] and small[7–9] angular scales, but only upper limits on the CMB polarization (CMBP) have been set up to now. In spite of its

Further author information: (Send correspondence to E.C.)
E.C.: E-mail: carretti@bo.iasf.cnr.it, Telephone: +39 051 6398735

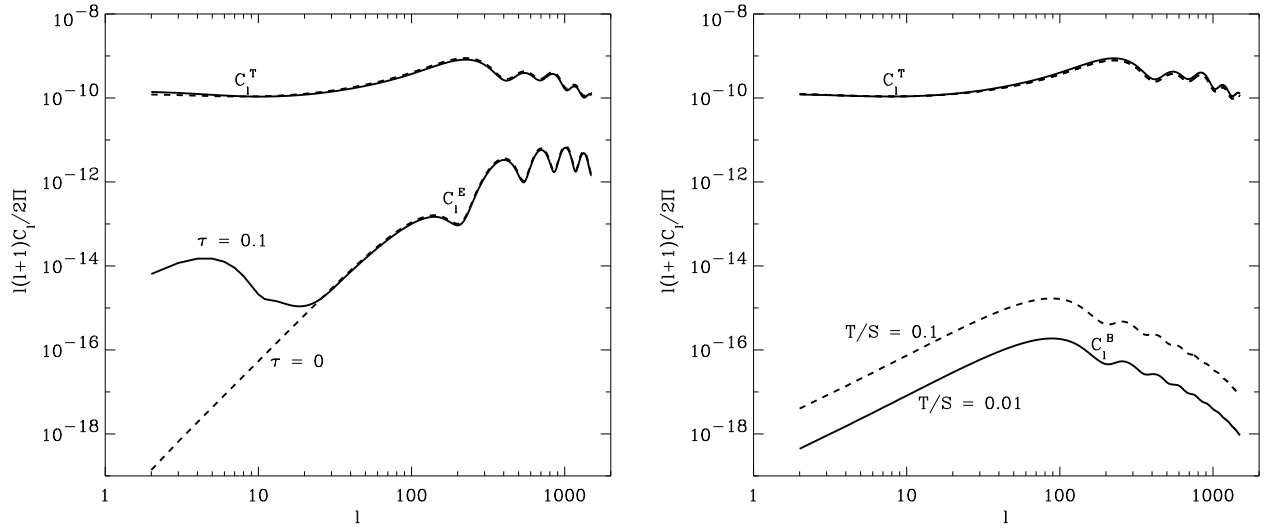

Figure 1. Left: Temperature anisotropy and E-mode power spectra. Two $\Omega_\Lambda = 0.7$ cosmological models which differ only in the re-ionization optical depth τ are shown. **Right:** Temperature anisotropy and B-mode power spectra. Two $\Omega_\Lambda = 0.7$ cosmological models which differ only in the tensor (gravitational waves) to scalar perturbation ratio T/S are shown.

elusiveness, the CMB polarization promises to add information to the CMB anisotropy data: it will provide a direct measurement of cosmological parameters that CMB anisotropy alone is not able to determine.[3] The optical depth τ in the dark ages and the epoch $z_{\rm ri}$ at which the re-ionization occurred are directly measured by CMBP informing us the formation epoch of the first structures and their growth-rate. Figure 1 presents a comparison between temperature and polarization (E-mode) power spectra for two cosmological models, which differ only in the optical depth τ of the re-ionized medium. It is clear that the E-mode spectrum is much more sensitive to τ than the temperature spectrum and that these new information are found at large angular scales ($l < 10$, i.e. $\theta > 20^{\rm o}$). In addition, the E-mode of the CMBP brings important information also at subdegree angular scales, where the *coherent* primordial fluctuations predicted by Inflation leave fingerprints like a well defined Doppler peak pattern: The peaks in the T and E power spectra alternate. Thus, the detection of the CMBP at subdegree scales leads to an indirect check of the inflationary model.[10]

The detection of the B-mode (although very week) is even more exciting: its level is directly related to the tensor-to-scalar perturbation ratio T/S (see Figure 1), whose value, in turn, is related to the energy of the Universe at the inflation time.[11] Thus, the measurement of the B-mode allow the estimate of the energy at which the inflation occurred and the identification of the right model in the zoo of the existing ones.

Moreover, besides their intrinsic interest, τ, $z_{\rm ri}$ and T/S determinations further improve the precision on other cosmological parameters.

Unfortunately, the CMBP predicted level is very low (few μK on sub-degree scales and less than 1 μK at large scales). Current experimental upper limits are still one order of magnitude higher than the expected level.[12–22] and, even though more sensitive detectors are coming, CMBP measurements are biased by foreground subtraction. Besides its intrinsic interest, the Galaxy acts as a foreground for CMB experiments and only its accurate knowledge will allow measurements of CMB features (See Ref. 23–25 and references therein).

So far, observations have been carried out only at frequencies up to 2.7 GHz,[25–30] where the Galactic emission appeares to be dominated by synchrotron. Such observations either are widely undersampled[26] or cover narrow stripes around the Galactic Plane,[27–30] but a better estimate of the foreground contaminations can be done only through Galactic surveys at frequencies closer to the CMBP range.

2. THE SPORT EXPERIMENT

The Sky Polarization Observatory (SPOrt)* is aimed at filling the current gap in measurements of the diffuse polarized emission in the 22-90 GHz range. It is an Italian Space Agency (ASI) funded experiment and it has been selected by ESA to be flown on board the International Space Station (ISS) for a minimum lifetime of 18 months, starting from 2005 (see Figure 2). The SPOrt experiment, together with BaR-SPOrt, on-ground observations and technological activities, is part of the SPOrt Programme[31] aimed at detecting the CMBP.

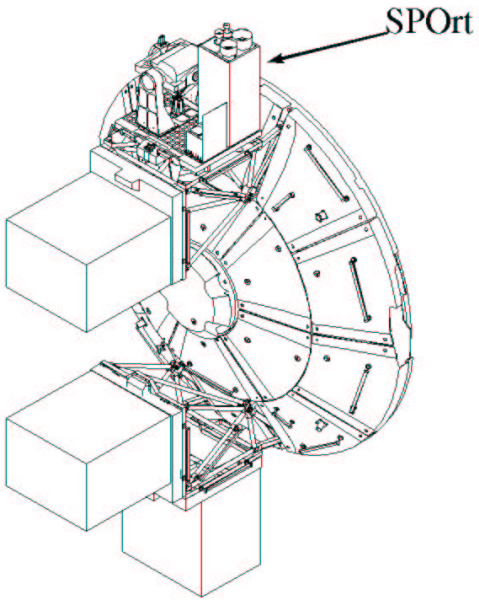

Figure 2. SPOrt position on the External Payload Facility of Columbus onboard the ISS (courtesy by Alenia Spazio)

SPOrt is the first space mission devoted to Q & U Stokes parameters measurements in the microwave domain at large angular scales ($\theta > 7^{o}$). This can be done only by all-sky surveys (space missions) and by instruments designed to be as much as possible insensitive to instrumental polarization.

The main features of SPOrt are the following (see also Table 1):

- multifrequency approch with four frequency channels at 22, 32, 60 and 90 GHz to match the best band for CMBP observation (90 GHz), while checking the Galactic contributions (22-90 GHz) and mapping the Galactic synchrotron emission (22 and 32 GHz).
- very simple optics (corrugated feed horns), providing angular resolutions down to 7°, suitable to access the new information on cosmological parameters contained in CMBP on large scales, while minimizing optics systematic effects.
- a nearly all-sky survey ($\sim 80\%$ sky coverage).

The CMBP signal is week (about 1-10% of CMBA, depending on the scale) requiring expressly devoted instruments, as CMBA does. Thus, great care has been taken to optimize the instrument design with respect to systematics generation, long term stability and observing time efficiency.

The following major choices were adopted for the SPOrt design:

*http://sport.bo.iasf.cnr.it

Table 1. SPOrt main features: σ_{1s} is the istantaneous sensitivity (1 second), σ_{PX} and $\sigma(P_{\rm rms})$ are the final sensitivity per pixel and for the $P_{\rm rms}$, respectively, considering a 18 month mission lifetime and 50% observing efficiency.

ν [GHz]	BW	FWHM	Orbit Time [s]	Coverage	N_{PX}	σ_{1s}[mKs$^{1/2}$]	$\sigma_{PX}[\mu$K]	$\sigma(P_{\rm rms})[\mu$K]
22, 32, 60, 90	10%	7°	5400	80%	660	1.0	5.2	0.3

1. correlation polarimeters to improve the stability (see Figure 3);
2. correlation of the two circularly polarized components E_L and E_R to directly and simultaneously measure both Q and U (100% observing time efficiency)

$$\begin{aligned} Q &\propto \Re(E_R E_L^*) \\ U &\propto \Im(E_R E_L^*) \end{aligned} \tag{1}$$

   This optimizes the sensitivity with respect to other schemes which provide either Q or U at once, just resulting in 50% efficiency (e.g. correlation or difference of the linear components);
3. detailed analysis of the correlation scheme to minimize the instrumental systematics by the identification of "critical" components and of the specifications they have to satisfy;
4. custom development of these components when the state-of-the-art were not enough.

3. DESIGN ANALYSIS

The radiometer equation[32, 33] helps us find the parameter to be controlled for minimizing systematic effects. In fact, in the expression[†]

$$\Delta T_{\rm rms} = \sqrt{\frac{k^2\, T_{\rm sys}^2}{\Delta\nu\, \tau} + T_{\rm offset}^2 \left(\frac{\Delta G}{G}\right)^2 + \Delta T_{\rm offset}^2} \tag{2}$$

the first term represents the white noise of an ideal and stable radiometer, while the second and the third terms are the gain and offset fluctuation effects, respectively, and represent the additional noise generated by instrument instabilities. The ideal behaviour is preserved provided that the offset is taken under control.

Correlation receivers are intrinsically more stable because of their lower offset generation. Figure 3 shows the scheme we adopted for the SPOrt radiometers. Polarizer and OMT extract the two circularly polarized components collected by a dual-polarization feed horn. After amplification, the two components are correlated by the correlation unit (CU). The latter includes an Hybrid Phase Discriminator (HPD), diodes and differential amplifiers, whose outputs are the two Stokes parameters Q & U.

In order to minimize the offset level an analysis has been carried out to identify the devices generating offset sources and the parameters to be controlled. The analysis shows the offset is generated at both CU and antenna system (horn, polarizer and OMT) levels.

The CU needs an HPD with high rejection of the unpolarized components. This has been achieved by the development of a custom device[35, 36] providing $>$ 30 dB rejection. In combination with a lock-in system, this makes negligible the CU contribution to the offset, being the total rejection $>$ 60 dB.

[†] $T_{\rm sys}$, $T_{\rm offset}$ and $\Delta T_{\rm offset}$ are the system temperature, the offset equivalent temperature and its fluctuation, respectively; G is the radiometer gain, τ the integration time, $\Delta\nu$ the radiofrequency bandwidth and k a constant depending on the radiometer type.

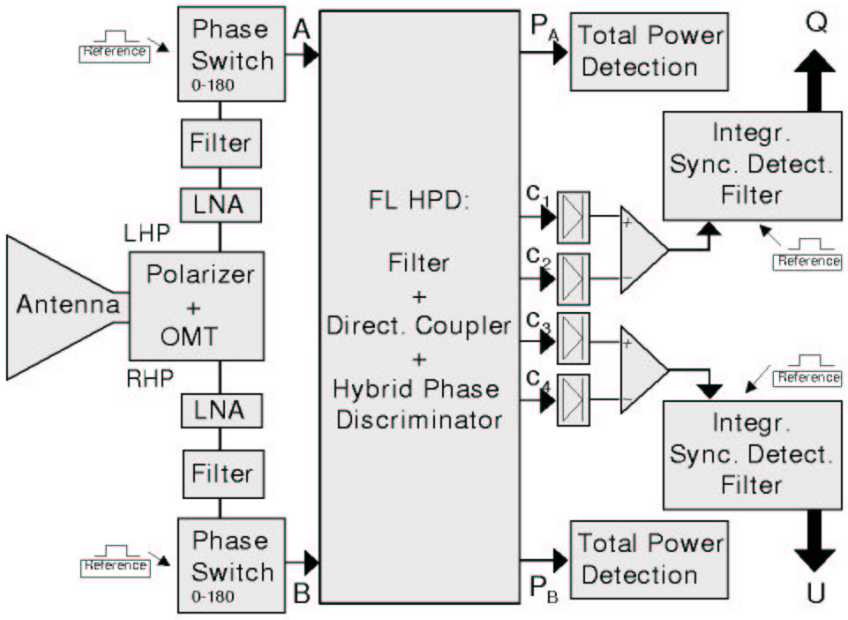

Figure 3. Schematic block diagram of the SPOrt radiometers. Polarizer and OMT extract the two circularly polarized components LHP & RHP collected by the horn. After amplification, the correlation unit (based on a Hybrid Phase Discriminator, see[35,36] for details) provides directly both Q & U.

Consequently, the antenna system is the most important offset source. Carretti et al. in Ref. 34 found that:[‡]

$$T_{\rm offset} = SP_{\rm OMT}\left(T_{\rm sky} + T^{\rm Ant}_{\rm noise}\right) + SP_{\rm pol}\left(T_{\rm sky} + T^{\rm horn}_{\rm noise} - \frac{T^{\rm pol}_{\rm ph}}{\eta}\right), \tag{3}$$

where the two quantities

$$SP_{\rm OMT} = 2\,\frac{\Re(S_{A1}S^*_{B1})}{|S_{A1}|^2}, \tag{4}$$

$$SP_{\rm pol} = \frac{1}{2}\left(1 - \frac{|S_\perp|^2}{|S_\parallel|^2}\right), \tag{5}$$

describe the goodness of the OMT and of the polarizer, respectively, from the offset generation point of view. Uncorrelated signals (noise and sky) are partially detected as correlated signals because of the OMT cross–talk (S_{A1} and S_{B1} are the transmission and cross-talk coefficient of the OMT, respectively) and of the polarizer attenuation difference ($S_\parallel$ and $S_\perp$ are the attenuations of the two polarization of the polarizer).

The instability of a radiometer can be measured in terms of the knee frequency ($f_{\rm knee}$), that provides the time scale at which the $1/f$ component of the noise power spectrum prevails on the white noise. Destriping techniques can remove most of the effects of the $1/f$ noise, but only if the knee frequency is lower than the signal modulation frequency.[37] For SPOrt this corresponds to the orbit frequency $f_{\rm orbit} = 1.8 \times 10^{-4}$ Hz.

Currently available InP Low Noise Amplifiers have rather high knee frequencies ($f^{\rm lna}_{\rm knee} \sim$ 100-1000 Hz), making correlation architectures more convenient. In fact, the knee frequency of a correlation receiver is related

[‡] $T_{\rm sky}$ is the signal collected from the sky, $T^{\rm horn}_{\rm noise}$ is the noise generated by the horn only, $T^{\rm Ant}_{\rm noise}$ is the noise temperature by the whole antenna system, η is the efficiency of the feed horn and $T^{\rm pol}_{\rm ph}$ is the physical temperature of the polarizer.

to that of its amplifiers by the formula

$$f_{\rm knee} = \left(\frac{T_{\rm offset}}{T_{\rm sys}}\right)^2 f_{\rm knee}^{\rm lna} \tag{6}$$

where $T_{\rm offset}$ is the radiometric offset and $T_{\rm sys}$ is the system temperature.

Equations (3)-(5) state that the main offset sources are the OMT cross-talk and the difference between the attenuations of the two polarizations of the polarizer. The SPOrt needs have been quantified in -60 dB and -30 dB, respectively, leading to an offset value as low as $T_{\rm offset} \sim 50$ mK which, combined with a $T_{\rm sys} \sim 100$ K, gives the knee frequency

$$f_{\rm knee} \sim 2.5 \times 10^{-7} f_{\rm knee}^{\rm lna} \tag{7}$$

matching the condition for a succesful destriping ($f_{\rm knee} < f_{\rm orbit}$)

However, state-of-the-art OMTs are not good enough, and custom hardware development has been required to the SPOrt team. Figure 4 shows the obtained result for the 32 GHz channel: a cross-talk as low as -70 dB has been achieved, well matching the -60 dB goal.

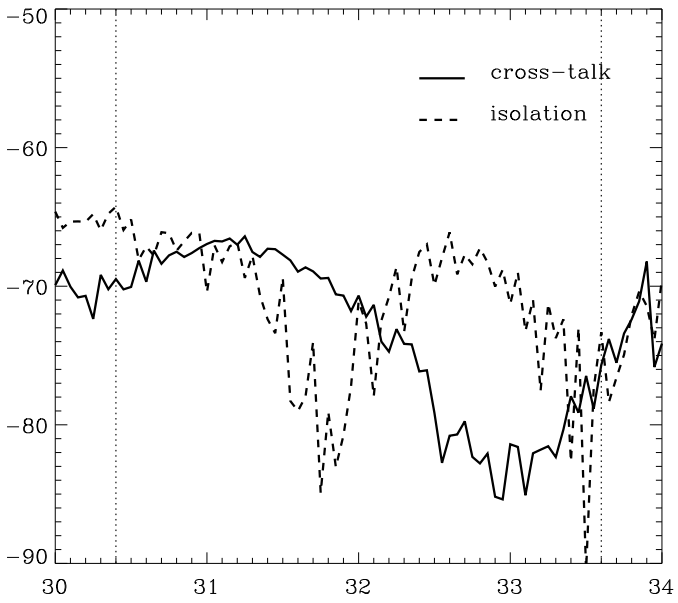

Figure 4. Magnitudes of both the isolation between the two rectangular ports and the cross-talk between the two polarizations for the 32 GHz SPOrt OMT. The vertical dotted lines show the 10% band.

Besides the offset generation, the SPOrt team has identified another systematic error source: the spurious polarization generated by the optics.[34] This is due to the anisotropy distribution of the unpolarized radiation modulated by the f pattern:

$$T^{\rm horn} = \frac{1}{\Omega_A}\int_0^{\pi} \sin\theta\, d\theta \int_0^{\pi/2} d\phi\, [\Delta T_b(\theta,\phi) - \Delta T_b(\theta,\phi+\pi/2) + \Delta T_b(\theta,\phi+\pi) - \Delta T_b(\theta,\phi+3/2\pi)] \cdot f(\theta,\phi)\,, \tag{8}$$

$$f(\theta,\phi) = -P(\theta,\phi)\chi^*(\theta,\phi+\pi/2) + \chi(\theta,\phi)P^*(\theta,\phi+\pi/2)\,, \tag{9}$$

where P and χ are the co-polar and cross-polar patterns, respectively, and Ω_A is the antenna beam. In the case of SPOrt feed horns, the contribution of the f pattern is ~ -24 dB and the rms contamination from the

30 μK of the CMB anisotropy is lower than 0.2 μK. Due to its intrinsic asimmetry, off-axis optics with the same cross-polar pattern level would imply a spurious contribution 8-10 dB higher.

Moreover, also the hardware calibration of a CMBP experiment represents a challenge. Standard marker injectors are not suitable for calibrating a tensorial quantity as the couple (Q, U) is. Thus, a new concept calibrator has been developed, valid for any radio-polarimeter, based on the insertion of three signals at different position angles. This device is similar to that of BaR-SPOrt and further details can be found in Ref. 38, 39.

In summary, the faint CMBP signal requires specifically devoted instruments and the SPOrt team has spent (and it is still spending) a big effort in designing an instrument with very low systematic error contamination, characterized by:

- correlation unit with high rejection of the unpolarized component (> 60 dB) based on a custom-developed HPD and a lock-in system;
- on axis and simple optics (corrugated feed horns) in order to minimize the spurious polarization induced by both the f pattern and the CMB temperature anisotropy at the beam scale: With such a configuration ~ -35 dB of cross-polarization translates into a contamination < 0.2 μK;
- high OMT isolation (> 60 dB) and low cross-talk (< -60 dB), since these parameters are among the major responsibles for Q & U offset generation in correlation polarimeters.
- very small difference (< -30 dB) between the attenuations of the two polarizations in the polarizer, which is the other main responsible for offset generation.

4. SCIENTIFIC GOALS

The goals of SPOrt are essentially two:

- provide 7° (HPBW) full maps of the Galactic synchrotron emission at 22-32 GHz;
- attempt a first detection of CMBP on large angular scales; more stringent upper limits (at least 1 order of magnitude lower than at present) have to be expected anyway.

The diffuse Galactic polarization, at frequencies greater than 2.7 GHz, is practically unknown. However, a level of $T_{\rm syn}(30\ {\rm GHz}) \sim 5\ \mu$K on 7° scales can be evaluated by down extrapolating data from Duncan et al..[27] Unpolarized data may provide an independent confirmation assuming, for example, a 30% of polarization in the COBE-DMR maps.

The expected scenario is sketched in Figure 5, where the CMBP is plotted together with the relevant foregrounds. The SPOrt sensitivities reported in Table 1 confirm that full maps of the Galaxy should be done at 22 and 32 GHz, following predictions.

However, since the SPOrt pixel sensitivities do not envisage the possibility of getting to CMBP maps, only full-sky statistical analyses may provide an estimate of the mean polarized signal $P_{\rm rms} = \sqrt{\langle Q^2 + U^2 \rangle}$. Similarly to what has been done by PIQUE[21] and POLAR[22] groups and applying the flat spectrum analysis,[40] simulations have been done based on the SPOrt capabilities. They show that a detection shall be expected with an error $\sigma(P_{\rm rms}) = 0.3$ μK (1σ C.L.), taking into account the degradation from foreground subtraction.

Figure 4 of Ref. 41 shows the $P_{\rm rms}$ behaviour, with respect to τ, be almost independent of other cosmological parameters. That is, the detection of the $P_{\rm rms}$ on large angular scales is relevant for a clean measurement of the optical depth of the reionized medium in the dark ages. A sensitivity of $\Delta\tau = 0.13$ for a model with $\tau = 0.2$ has been determined through a Fisher matrix analysis.

ACKNOWLEDGMENTS

We thank V. Natale for useful discussions. We acknowledge use of CMBFAST package for performing our analysis. SPOrt is an ASI funded project. We thank also ESA for provding the flight opportunity onboard the International Space Station.

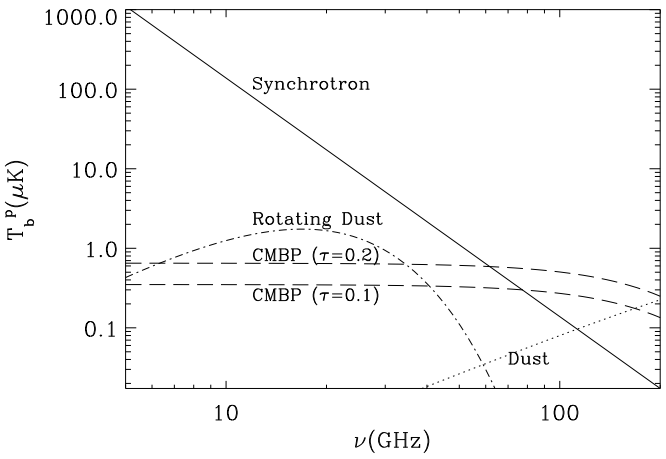

Figure 5. Expected polarized brightness temperature for the relevant polarized Galactic foregrounds on 7° scale. The synchrotron emission has been normalized to $T_{\rm syn}(30\ {\rm GHz}) \sim 5\,\mu$K: See text for details. The parameters of the other components are from Tegmark et al..[24] The CMBP behaviour for two ΛCDM models ($\Omega_\Lambda = 0.7$) with optical depth $\tau = 0.05$ is also shown.

REFERENCES

1. Sazhin M. V., Benitez N., *Astrophys. Lett. Commun.* **32**, 105, 1995.
2. Jungman G., Kamionkowski M., Kosowsky A., Spergel D. N., *PRD* **54**, 1332-1344, 1996.
3. Zaldarriaga M., Spergel D. N., Seljak U., *ApJ* **488**, 1, 1997
4. Efstathiou G., Bond J. R., *MNRAS* **304**, 75, 1999.
5. Smoot G.F., et al., *ApJ* **396**, L1, 1991.
6. Bennet C.L., et al., *ApJ* **464**, L1, 1996.
7. De Bernardis P., et al., *Nature* **404**, 955, 2000.
8. Hanany S., et al., *ApJ* **545**, L5, 2000.
9. Miller A. D., et al., *ApJ* **524**, L1, 1999.
10. Kosowsky A., *NewAR* **43**, 157-168, 1999.
11. Kamionkowski M., Kosowsky A., *PRD* **57**, 685, 1998.
12. Penzias A. A., and Wilson R. W., *ApJ* **142**, 419-221, 1965.
13. Caderni N., et al., *Phys. Rev. D* **17**, 1901-1907, 1978.
14. Nanos G. N., *ApJ* **232**, 341-347, 1979.
15. Lubin P. M., and Smoot G. F., *ApJ* **245**, 1-17, 1981.
16. Partridge R. B., et al., *Nature* **331**, 146-147, 1988.
17. Wollack E. J., et al., *ApJ* **419**, L49-L52, 1993.
18. Netterfield C. B., et al., *ApJ* **445**, L69-L72, 1995.
19. Sironi G., Boella G., Bonelli G., Brunetti L., Cavaliere F., Gervasi M., Giardino G., Passerini A., *NewA* **3**, 1-13, 1998.
20. Subrahmanyan R. et al., *MNRAS* **315**, 808-822, 2000.
21. Hedman M. M. et al., *ApJ* **548**, L111-L114, 2001.
22. Keating B. G., et al., *ApJ* **560**, L1, 2001.
23. Tucci M., Carretti E., Cecchini S., Fabbri R., Orsini M., Pierpaoli E., *NewA* **5**, 181, 2000.
24. Tegmark M., Eisenstein D. J., Hu W., de Oliveira–Costa A., *ApJ* **530**, 133, 2000.
25. Bruscoli M., Natale V., Tucci M., Carretti E., Fabbri R., Cortiglioni S., Sbarra C., *NewA* **7**, 171, 2002.

26. Brouw W. N., Spoelstra T. A. Th., *A&AS* **26**, 129, 1976.
27. Duncan A. R., Haynes R. F., Jones K. L., Stewart R. T., *MNRAS* **291**, 279, 1997.
28. Duncan A. R., Reich P., Reich W., Fürst E., 1999, *A&A* **350**, 447, 1999.
29. Uyaniker B., Fürst E., Reich W., Reich P., Wielebinski R., *A&AS* **138**, 31, 1999.
30. Gaensler B. M., Dickey J. M., McClure–Griffiths N. M., Green A. J., Wieringa M. H., Haynes R. F., *ApJ* **549**, 959, 2001.
31. Cortiglioni S., et al., in *AMiBA 2001: High-z Clusters, Missing Baryons, and CMB Polarization*, *ASP Conf. Ser.* **CS-257**, in press, 2002
32. Wollack E.J., *Rev. Sci. Instrum.* **66**, 4305, 1995
33. Wollack E.J., Pospieszalski M.W., *IEEE MTT-S Digest 1998*, p. 669, 1998
34. Carretti E., Tascone R., Cortiglioni S., Monari J., Orsini M., *NewA* **6**, 173-187, 2001 (*astro-ph*/0103318).
35. Tascone R., Trinchero D., Baralis M., Peverini O.A., Olivieri A., Carretti E., Cortiglioni S., in *Experimental Cosmology at Millimetre Wavelengths*, *AIP Conf. Proc.* **616**, 150, 2002.
36. Peverini O.A., Baralis M., Tascone R., Trinchero D., Olivieri A., Carretti E., Cortiglioni S., in *Astrophysical Polarized Backgrounds*, *AIP Conf. Proc.* **609**, 177, 2002.
37. Sbarra C., Carretti E., Cortiglioni S., Zannoni M., Fabbri R., Macculi C., Tucci M., in *Astrophysical Polarized Backgrounds*, *AIP Conf. Proc.* **609**, 193, 2002.
38. Baralis M., et al., in *Astrophysical Polarized Backgrounds*, *AIP Conf. Proc.* **609**, 257, 2002.
39. Zannoni M., et al., *this volume*, 2002.
40. Zaldarriaga M., *ApJ* **503**, 1, 1998.
41. Carretti E., et al., in *Astrophysical Polarized Backgrounds*, *AIP Conf. Proc.* **609**, 109, 2002.